Bayesian Inference for Heterogeneous Caprock Permeability Based on Above Zone Pressure Monitoring

Argha Namhata[1, 2, *], Mitchell J. Small[1], Robert M. Dilmore[2], David V. Nakles[1], Seth King[3]

1 Department of Civil & Environmental Engineering, Carnegie Mellon University, Pittsburgh, PA 15217, USA

2 U.S. Department of Energy, National Energy Technology Laboratory, 626 Cochrans Mill Road, Pittsburgh, Pennsylvania 15236, USA

3 U.S. Department of Energy, National Energy Technology Laboratory, AECOM, 3610 Collins Ferry Road, Morgantown, WV 26507

** Corresponding Author: Email: anamhata@andrew.cmu.edu (A. Namhata), Tel: +1 (412) 370-4671.*

ABSTRACT

The presence of faults/ fractures or highly permeable zones in the primary sealing caprock of a CO_2 storage reservoir can result in leakage of CO_2. Monitoring of leakage requires the capability to detect and resolve the onset, location, and volume of leakage in a systematic and timely manner. Pressure-based monitoring possesses such capabilities. This study demonstrates a basis for monitoring network design based on the characterization of CO_2 leakage scenarios through an assessment of the integrity and permeability of the caprock inferred from above zone pressure measurements. Four representative heterogeneous fractured seal types are characterized to demonstrate seal permeability ranging from highly permeable to impermeable. Based on Bayesian classification theory, the probability of each fractured caprock scenario given above zone pressure measurements with measurement error is inferred. The sensitivity to injection rate and caprock thickness is also evaluated and the probability of proper classification is calculated. The time required to distinguish between above zone pressure outcomes and the associated leakage scenarios is also computed.

1. INTRODUCTION

CO_2 capture and storage (CCS) is considered a promising strategy for the reduction of anthropogenic greenhouse gas emissions to the atmosphere (IPCC, 2005). However, injecting large volumes of CO_2 may cause subsurface pressurization over large spatial domains, resulting in leakage that returns the injected CO_2 to the atmosphere and potentially harming natural resources (e.g., groundwater resources) (Birkholzer and Zhou, 2009; Pruess, 2004). To protect the environment and public health, a comprehensive risk profile should be established for each CCS project. To monitor these risks, it is necessary to have the capability to identify and resolve the onset, location, and volume of leakage from the reservoir in a systematic and timely manner. The monitoring of pressure changes, as an indication of leakage, represents one approach to provide this information, and has been explored by a number of investigators (Nogues et al., 2011; Sun and Nicot, 2012; Zeidouni and Pooladi-Darvish, 2012; Benisch and Bauer, 2013; Hovorka et al., 2013; Jung et al., 2013; Strandli and Benson, 2013; Azzolina et al. 2014; Wang and Small, 2014). In many of these studies highly simplified conceptual models have been used for the affected subsurface layers, including an assumption of homogeneous porosity and permeability in each (though in several cases the single values for each zone are treated as uncertain inputs to the model). In this paper, we maintain an idealized geometry for the subsurface system, but incorporate heterogeneity in the fracture pattern of the caprock and its resulting location-specific effective permeability. In addition, we apply a probabilistic approach in which uncertainty in the subsurface may be resolved by successive monitoring results.

Monitoring for leak detection at CO_2 storage sites serves a number of purposes, including ongoing assurance that the site is maintaining its integrity, verification that credited quantities of stored CO_2 do in fact remain underground, and alerting operators when changes are needed to modify or stop operations, including possible initiation of more intensive monitoring and remediation. Subsurface models complement monitoring by allowing interpretation of the observed data to identify the location and size of possible leakage sources, and to predict the subsequent costs and risks of alternative response options (see, for example, Gerstenberger and Christophersen, 2016). Models that consider the performance of both the subsurface system and the monitoring network are especially useful in this regard, allowing a pre-construction estimate of the performance of alternative monitoring technologies and network designs under plausible leakage scenarios, including overall false positive and false negative rates for system-wide leak detection (Yang et al. 2011, 2012). Once such performance models have been developed and applied, they may be used for optimization of a monitoring network, as previously shown for near-surface groundwater leak detection (e.g., Loaiciga, 1989; Loaiciga et al., 1992; Meyer et al., 1994; Mahar and Datta, 1997; Reed and Minsker, 2004; Dhar and Datta, 2007). Similar optimization approaches have recently been proposed for the design of CO_2 leakage detection networks (Sun et al., 2013; Yonkofski et al., 2016).

Pressure monitoring in the Above Zone Monitoring Interval, or AZMI, has been proposed for early detection of leakage (Hovorka et al., 2013) because of the fast traveling speed of pressure perturbations and the proximity of the AZMI to storage formations (Nordbotten et al., 2004). However, unlike the storage formations, the AZMI will be subjected to less pressure disturbance during injection activities, which will require a monitoring network capable of detecting these smaller signals as well as interpreting potential anomalous pressure signals. From an operations perspective, deep pressure monitoring wells are costly to drill and maintain—drilling and instrumentation costs can easily exceed \$ 1 million per well, which is in addition to annual maintenance and operation costs (U.S. Environmental Protection Agency, 2010). Thus, there is strong incentive to optimize the design of pressure-based monitoring networks (Sun et al., 2013).

In this paper, we focus on leakage of CO_2 through the primary caprock and resulting pressure changes in the AZMI. The primary aim of this work is to characterize the time required to distinguish AZMI pressure outcomes and associated leakage scenarios through a probabilistic assessment of the integrity and permeability of the caprock and also the amount of CO_2 injected into the reservoir. We present a method for integrating monitoring and modeling results to draw inferences regarding the integrity of the caprock, including how quickly these inferences can be made for different representative caprock types and conditions. These scenarios represent effective caprock permeability from almost impermeable to highly permeable cases. We then model the probability distributions of pressure build-up in the AZMI for each of these scenarios, with the modeled pressure fields assumed to be observed with measurement errors. These distributions serve as the likelihood function for a Bayesian classification model, in which the posterior probabilities are computed for each of the four caprock fracture scenarios. We also evaluate the influence of the thickness of the caprock and the CO_2 injection rate on the modeled pressure build-up and the subsequent performance of the Bayesian classification procedure. The modeling approach used in this study is based on the systematic framework shown in Figure 1. The results from this work can in the future form the basis for more refined evaluation and optimization of monitoring technologies and networks.

2. MODEL SETUP

The CO_2 storage system is modeled as a three-layer system with two aquifers separated by a sealing caprock of thickness 50 m (Figure 2 (a)). The lower aquifer is the storage reservoir where CO_2 is injected at a base case rate of 1 MT per year for a period of 30 years. Higher and lower injection rates are also considered in a sensitivity analysis. The base case thickness of the reservoir is assumed to be 100 m. The reservoir is located at a depth of 1000 m. The areal extent of the subsurface storage system is defined as 10 km × 10 km. The assumed reservoir features are summarized in Table 1. Reservoir simulations (Figure 3) are conducted using TOUGH2. CO_2 and brine flux from the seal are then simulated for a period of 30 years of injection and 170 years of post-injection using the seal model, NSealR (Lindner et al., 2015). NSealR is a reduced order model (ROM) developed by the U.S. Department of Energy's National Risk Assessment Partnership (NRAP) program (NETL, 2011). NSealR uses a two-phase, relative permeability approach with Darcy's law for one dimensional (1-D) flow computations of CO_2 through the horizon in the vertical direction. The above zone thickness used in this study is 50 m. It is assumed that the AZMI layer has a porosity of 0.1 and a permeability of 10.5 mD. The residual CO_2 and brine saturations were set at 0.01 and 0.02 respectively and the bubbling pressure was set to equal

0.01 MPa. Three base case observation wells screened at 900 m depth are also considered. The locations of the wells are shown in Figure 2 (b). The locations are chosen to be representative of a possible spatial layout, primarily for demonstration purposes.

The sealing caprock is modeled for four different fractured network scenarios: (I) fractured network with low aperture; (II) randomly distributed clusters of fractures with high apertures; (III) fractured network zone with high aperture near the injection well and; (IV) densely fractured network with high aperture. These four scenarios are assumed to be representative of the range of possible storage seal scenarios with an impermeable seal layer with almost no leakage possible represented by scenario (I); permeable and high risk storage scenarios represented by scenarios (III) and (IV) and a high integrity, almost impermeable seal with low leakage risk represented by scenario (II).

2.1. FRACTURED SEAL SCENARIOS

Quantitative assessment of storage system performance suggests that safe, effective long-term containment is highly probable in cases where there is an in-tact low-permeability seal to prevent vertical fluid migration. To date, however, little consideration has been given to scenarios in which the primary sealing layer contains regions fracturing or faulting that effectively represent heterogeneities in seal permeability. In this model, the sealing caprock is considered to be 50 m thick. In order to add heterogeneity to our analysis, we simulate semi-stochastic fracture network characteristics using FRACGEN (McKoy et al., 2006). This software is specifically designed for modeling fracture networks and fractured reservoirs. The fracture network used in this model is based on the stochastic allocation of fracture lengths, positions, orientations and density in space. Model details are provided in the *Supporting Information*.

To demonstrate the overall methodology, we have chosen four possible fracture scenarios as represented graphically in Figure 4 to provide a discrete sample from a range of plausible caprock types with varying susceptibility to leakage. In this regard the four scenarios can be thought of as representative of alternative conceptual models for the caprock system.

Fracture modeling details used in each of these scenarios can be found in *Table S-2 of the Supporting Information*. The four seal scenarios generated for this work are expected to be representative of fractured seal scenarios ranging from an almost impermeable caprock layer (good storage seal case) to a highly permeable caprock layer (worst storage seal case). These scenarios are intended to illustrate how alternative seal fracture properties can be defined, simulated, and used to induce a leakage and fluid migration pattern from the injection zone, through the caprock and into the AZMI. Since the NSealR model uses seal permeability as an input, we use a parallel plate model for fractures to compute the effective permeability of the fractured networks. More refined uncertainty analysis could be explored by allowing prior parameter values (e.g., fracture properties) to be uncertain for each scenario, with observations providing simultaneous updating of parameter distributions and model probabilities, as is done in Bayesian model discrimination and Bayesian model averaging (Hoeting et al., 1999; Wintle et al., 2003).

Application of Bayesian model averaging to groundwater modeling with uncertain conceptual models and scenarios is found in Meyer et al. (2007), Rojas et al. (2008, 2010) and Ye et al. (2010). In these applications, no single model is assumed to be "true", nor is the set of models assumed to be exhaustive of all possibilities. Rather the prior and posterior probabilities for each model are understood in a relative sense (as would be "weights" in a model averaging calculation), and this is the context in which we interpret the calculated posterior probabilities for the set of scenarios considered. Indeed, the purpose is to see when an inference can be made with a high level of surety that one scenario (or combination of scenarios, especially those including scenarios conducive to leakage) is more likely than others, and not the determination of exact probabilities for each. In practice, selection of alternative scenarios would consider all available information for a site (i.e., providing an "informed prior"), and would cover the full range of possible conceptual models that could inform the level of leakage risk. Meyer et al. (2007), Rojas et al. (2008), Rojas et al. (2010) and Ye et al. (2010) demonstrate model sets of 8, 3, 7, and 25 model scenarios, respectively. It is likely that application of the proposed leak detection methodology at actual, complex sites will involve the consideration of significantly more than four conceptual alternatives.

2.2. EFFECTIVE CAPROCK PERMEABILITY

Defining the aperture and the permeability of a fracture separately seems counterintuitive, since these parameters are considered to be mutually dependent, and directly related if the fractures are rectangular slits. Parallel plate theory (Snow, 1964; Sarkar, 2004) is used to compute fracture permeability (*See Supporting Information*). Figure 5 shows the effective permeability plot for the four fractured scenarios. The calculated permeabilities are then used to compute flow through the seal using NSealR. While fracture flow is advective at the scale of individual pores and fractures, it is represented as a diffusive flux, characterized by permeabilities and pressure gradients at the spatial grid scale of the model. As this study focuses on the above zone pressure build up due to associated CO_2 leakage through the primary caprock, we determine whether the four-different fractured caprock scenarios lead to pressure build up profiles that are statistically distinguishable (Table 2).

2.3. AZMI MODEL RESULTS

The AZMI ROM (Namhata et al., 2016) is used to calculate the above zone pressure build up for each of the caprock scenarios. Figure 6 presents the changes in pressure responses in the AZMI over time, generated using the flux from the seal for each of the fracture scenarios for the simulation periods previously identified.

3. BAYESIAN CLASSIFICATION METHODOLOGY

An expert's belief regarding the relative probability that each caprock fracture scenario is present at a site can be combined with observed pressure monitoring and modeling results using Bayesian classification theory. The belief of the expert is assumed to be a prior distribution of the presence of each of the four scenarios at a CO_2 storage site. In the Bayesian classification methodology, the posterior distribution is then derived by combining the prior distribution with the monitored pressure at the three monitoring locations. If there is no information on the prior distribution, an equally probable prior is assumed so that the results will totally depend on the monitored (or, modeled) pressure outputs. In this case, the posterior probability of a fracture scenario is proportional to the likelihood function for the modeled pressure outputs (time and location dependent), given each fracture scenario.

To characterize the performance of the classification procedure, simulated leakage – pressure outcomes are generated for each scenario and translated into an assumed sequence of AZMI pressure measurements. The likelihood function for the above zone pressure measurements using the AZMI ROM has two components: firstly, the uncertainty in the true value of the above zone pressure that results from uncertainties in caprock fracture properties; and secondly, the uncertainty that might be associated with the modeling error. The first uncertainty is captured by 100 discrete FRACGEN simulation results. The latter is captured by assuming log normal measurement error function that maps simulated modeling results to pressure values that are assumed to be measured. To determine the ability to infer true caprock fracture scenario type at the site, we simulate multiple realizations for each fracture scenario, assume they are measured with error, and use the Bayesian classification procedure to infer the probability that each scenario is present. Good performance occurs when the procedure predicts high probability for the scenario used to simulate the leakage and associated pressure realizations (and low probability for the others).

3.1. Mean Pressure Buildup

As shown in Figure 2 (b), we have assigned three above zone monitoring wells for our base case analysis. The number and location of the monitoring wells chosen in this study are illustrative. The regions closer to the injection well are expected to see higher pressure build up, making them an obvious choice for monitoring. The three locations chosen are in regions right above or near the injection well. In this analysis, we calculate the above zone pressure build up due to CO_2 injection in the storage reservoir for each of the fractured seal scenarios (Figure 6). The pressure build ups at the three monitoring locations are then calculated for each scenarios and at each time step. The mean of the monitored pressure build up is then used for the analysis. The purpose of choosing the mean pressure build up ($\Delta P_{simulated}$) over individual monitoring point analysis is that it provides the ability of the mean pressure build up to capture the spatial variability in output predictions over individual analysis. The mean pressure build up range from the 100 simulations for each scenario is shown in Figure 7.

3.2. Inferring Fracture Scenario

Assuming no knowledge about the seal, we assign equal prior probability (= 0.25) for each of the four fracture scenarios (Table 2). This approach is commonly utilized in multi-model Bayesian analysis, ensuring that the alternatives begin on an equal footing and allowing the observations to provide the differentiating evidence for changes in their relative weights in the posterior distribution. At actual site applications, the full set of geologic site characterization data and expert knowledge can be utilized to inform prior probabilities (Gerstenberger and Christophersen, 2016). The mean above zone pressure build up in the three monitoring wells ($\Delta P_{simulated}$) is chosen to be the variable for analysis of the fracture seal scenarios. The expected effective permeabilities of the caprock for each of the fracture scenarios are shown in Table 2. The greater the effective permeability of the seal, the more will be the pressure build up in the AZMI resulting in higher $\Delta P_{simulated}$. For the cases considered and simulated in our study, the $\Delta P_{simulated}$ ranges from 0 to 0.325 MPa. Since we consider measurement errors, the observed values tend to extend beyond this range. For simplicity in the statistical analysis (mainly for lognormal analysis), we add a minimum threshold value of 0.001 MPa to the ΔPsimulated.

We then estimate the likelihood of observing $\Delta P_{simulated}$ given each caprock fracture scenario, $f(\Delta P_{simulated} \mid Scenario\ j)$, where j is the scenario number. We first generate 100 realizations of each caprock fracture scenario incorporating values shown in Table 1, and compute $\Delta P_{simulated}$. Secondly, we simulate the effects of measurement errors, by assuming that the above zone pressure build ups ($\Delta P_{measured}$) are log-normally distributed about the model simulation values:

(1)

$\Delta P_{measured} \sim \text{lognormal } (a, b)$

where,

$a = \log(\Delta P_{simulated})$

$b = [\log(c.v.^2 + 1)]^{1/2}$

We calculate the median $\Delta P_{simulated}$ values from each FRACGEN simulation for the respective lognormal distributions of $\Delta P_{measured}$ (specifying the parameters a representing the logarithm of the median of the respective measurements). The lognormal distribution is commonly assumed for the distribution of measurement errors around a true value, particularly for quantities such as concentrations and (in this context) pressure increments, which are assumed to be non-negative (Sohn et al. 2000; Ramaswami et al. 2005; Wang and Small, 2014). The second parameter b represents the standard deviation of the logarithm of $\Delta P_{measured}$. These second parameters are specified by the coefficients of variation (*c.v.*) of $\Delta P_{measured}$. The lognormal distribution is reasonably approximated by a normal distribution when the *c.v.* of the error is low, and a normal error distribution has also been used for pressure measurements in previous studies (e.g., Gavalas et al. 1976).

Thus, the lognormal distribution of $\Delta P_{measured}$ is computed using the simulation results of $\Delta P_{simulated}|i$ for each simulation i and at each time step t and the assumed measurement error (coefficient of variation here) for each $\Delta P_{simulated}$ measurement (determined by b). The pdf of the lognormal distribution serves as the likelihood function for the pressure observations given the simulation result:

$$f(\Delta P_{measured}(t)|a_i, b) = \log\left(\frac{1}{\Delta P_{measured}(t) \times a_i \times \sqrt{2\pi}} \exp\left\{\frac{-(\log(\Delta P_{measured}(t)) - a_i)^2}{2b^2}\right\}\right) \quad (2)$$

The overall log-likelihood of a given fracture scenario is given by the sum of individual log-likelihoods from all 100 simulations for each case:

$$\text{loglikelihood}(\text{scenario } j(t)) = \sum_{i=1}^{100} f(\Delta P_{measured}(t)|a_i, b) \quad (3)$$

Using Bayes theorem, the prior distribution of each caprock fracture scenario and the likelihood function are combined to calculate the posterior distribution of each caprock fracture scenario given by:

$$\pi(\text{scenario } j(t)|\Delta P_{measured}(t)) = \frac{\exp[f(\Delta P_{measured}(t)|scenario\ j)] \times \text{Prob[scenario } j]}{\sum_{i=1}^{4} \exp[f(\Delta P_{measured}(t)|scenario\ i)] \times \text{Prob[scenario } i]} \tag{4}$$

3.3. Time to Detect Leakage

The primary aim of this work is to compute the time required to distinguish between above zone pressure outcomes and the associated leakage scenarios. The time to detect leakage or no leakage are calculated using the posterior probabilities given each of the four scenarios. We compute two different time values, (a) the time to no leakage assurance given there is no leakage ($T_{no\ leak}$) and, (b) time to leakage confirmation given there is a leakage (T_{leak}). For simplicity, we assume that the fracture scenario I is a no leakage scenario. $T_{no\ leak}$ provides an assessment of the system behavior by calculating the time required to correctly conclude that there is leakage from the caprock assuming that the caprock is of scenario I type i.e., almost impermeable caprock. T_{leak} provides an estimate of how long it takes to correctly conclude that there is leakage from the caprock assuming that the caprock is of scenario types II, III or IV. Posterior probability thresholds of 90% are assumed to be required for drawing the no-leak or leak scenario inferences. Mathematically,

$$T_{no\ leak} = t,\ \text{when}, \pi([\text{scenario I}(t)|\Delta P_{measured}(t)] \geq 0.9|\text{scenario I}(t)) \tag{5}$$

and,

$$T_{leak} = t, \text{when}, \pi(\big[\text{scenario I}(t)|\Delta P_{measured}(t)] < 0.9|\text{scenario } j(t)\big): j \neq \text{I} \tag{6}$$

3.4. Influence of Input Parameters

Along with the uncertainties in fracture properties (represented in *Table S-2, See Supporting Information*), there can be other uncertainties associated with a CO_2 storage system that impact the above zone pressure monitoring results. To illustrate the sensitivity of model predictions to variations in selected modeling parameters, we change the CO_2 injection rate and thickness of the primary caprock to compute their effect on simulation results and the probability of properly inferring caprock fracture scenarios. The base case model was set up for a caprock of thickness 50 m and an injection rate of 1 MT/ year for 30 years. We make changes to the base case and also present simulation results for a 10 m and 100 m thick caprock; and injection rates of 10 MT/ year and 50 MT/ year.

4. RESULTS

The base case model was implemented for each of the four caprock fracture scenarios. The above zone pressure buildup was then calculated using the AZMI ROM. For posterior analysis we use the mean pressure buildup from three monitoring well locations as described previously. Figure 8 shows the posterior probability of each of the caprock fracture scenarios as a function of time from the start of injection. The posterior probabilities are calculated for each of the fracture scenarios given the simulation results from a particular fracture scenario. This demonstrates whether and how quickly a true fracture scenario can be distinguished from the others considered, based solely on pressure measurements in the AZMI. Since the fracture scenarios are general in nature, chosen to be representative of probable caprock types with different leakage potential, the results are intended to provide a simple representation of how the monitored pressure will evolve and be interpreted for similar scenarios.

In Figure 8, we present the posterior distribution of each scenario given one of the four scenarios. All of the plots have been shown until 35 years from the start of injection. Since the main aim of this work is to identify the time required to distinguish above zone pressure outcomes and the associated leakage scenarios, we concluded from all the simulations that the maximum associated time is less than 35 years. In each of the plots, there is no change in posterior probability from the prior values (= 0.25) in the first 3 years. It can be seen from the scenario I plot that the posterior probability of scenario I given scenario I reaches 0.90 at 5 years from the start of injection. This is expected because with more and more monitoring, the posterior probability is expected to increase for a particular scenario given the same scenario. A similar trend is expected for the other scenarios, but they take longer to reach a statistically significant posterior probability (= 0.90). While the leakage scenarios can, as a group, be distinguished from the non-leakage case, the method is often unable to distinguish the scenarios from each other. This is because there is no flow of CO_2 in the initial years to the AZMI, resulting in no pressure buildup. Scenario I being distinctively different from the rest of the scenarios has a very distinct posterior pattern. Since this scenario represents a negligible leakage case, we don't see the posterior of other scenarios, especially scenarios III and IV, increasing. Scenario II being a low leakage case, there will be no/ very less migration of fluids, hence there is a slight increase in its posterior initially.

For posterior probability plots of scenarios III and IV given scenarios III and IV respectively, there is an increasing trend as these scenarios are representative of high leakage cases, with almost no leakage effect from scenario I and very low impact from scenario II. Given scenario III, we see an increase in the posterior probability of scenarios II and IV at a later stage of injection since both these scenarios also have increasing pressure buildup over time. But the posteriors remain less compared to the posterior of scenario III. In case of scenario II, which is representative of low permeability caprock with the potential for a low to moderate amount of CO_2 leakage, we see higher probability of scenario I compared to scenario II itself in the first 5 years. The reason being in its initial years, there is negligible leakage of CO_2 in scenario II, similar to that of scenario I. So there is a clear impact on posteriors for that case.

We next conducted sensitivity analysis to determine the effect of changing caprock thickness (from a base case of 50 m) and the injection rate (from a base case of 1 MT/ year) on model inferences to:

(a) Caprock thickness of 10 m and 100 m

(b) Injection rate of 0.25 MT/ year and 5 MT/ year.

Figures 9 and 10 shows the inferred posterior probabilities over time for caprock thickness 10 m and 100 m, respectively, keeping all the other inputs to the simulation the same as the base case simulation. Figures 11 and 12 shows the posterior distribution over time for injection rate of 0.25 MT/ year and 5 MT/ year, respectively, for 30 years. From Figures 9 and 10 it can be seen that the general characteristic trend of the posteriors are similar to that in Figure 8. With a decrease in caprock thickness to 10 m (Figure 9), there will be more leakage of CO_2 in the AZMI compared to that from a caprock of thickness 50 m. This distinctive feature is captured for posteriors given scenario II plot, where the time to predict confidently that the change in pressure is due to scenario II is increased from the base case. For scenario III and IV, which are in general high leakage scenarios, the pattern is similar to that of the base case. When the caprock thickness is increased to 100 m (Figure 10), we expect lower CO_2 leakage into the AZMI compared to that of the base case. In this case too, scenario II cannot be distinguished from scenario I as quickly as the rest of the scenarios. Comparing the curves in Figures 9 and 10 to that of 11 suggests that changing the caprock thickness has very little effect on the magnitude of predicted probabilities. This is not the case when we change the injection rates. A lowering of the injection rates yields a lower or similar statistical ability to infer the caprock fracture scenario compared to that of the base case. Increasing the injection rate (Figure 11) yields an increase in the statistical ability for inferring the caprock fracture scenario. This is as expected – increasing the injection rate increases the likelihood of CO_2 leakage and in turn results in an increase in above zone pressures yielding a more likely detection of caprock fracture scenarios. The present model is formulated based on the assumption that there is no prior scenario-specific knowledge. In case of prior information about the caprock geology, the probability of inferring the caprock scenarios will also change. In this study, to show the impact of prior knowledge on caprock type inference and also the time taken to detect a leak/ no leak scenario, we slightly change the prior information situation from that of Table 2. The prior of Scenario I is changed to 0.50 and the rest of the scenarios are taken to have a 0.1667 prior probability. The resulting inferred posterior probabilities are shown in Figure 13. It can be seen that, with higher prior information of Scenario I, the posterior probability of Scenario I given Scenario I is quite high from the beginning. In the Scenario II plot it can be seen that the time to infer the leakage due to Scenario II has changed a lot. The other scenarios have almost similar inference ability to that of the base case.

As the primary aim of this work is to calculate $T_{no\ leak}$ and T_{leak}, we present the respective times for the base case and the four other scenarios in Tables 3 and 4. In Table 3, the time to no leak assurance is shown. This will help in understanding the minimum time required to confidently say that there are no significant monitorable pressure changes in the AZMI. The higher the caprock thickness and the lower the injection rate, more will be the time required to reach a no leak assurance conclusion since we expect to have low leakage in such situations. For an opposite scenario, with low caprock thickness and high injection rate, the time to no leak assurance will be much less. In Table 4, the time to leakage confirmation is shown. This is the time needed to conclude that most probably there is a leakage in the system based on the pressure data. The most time needed to conclude that there is a leakage in the system occurs with scenario II when the caprock thickness is low and the injection rate is low and medium. This occurs because, for such a scenario, there is expected to be much less leakage or no leakage. In order to reach a statistically significant conclusion that there is a chance of leakage, a long time is required. On the other hand, in scenario III where the fractured zones are above the injection well and below the monitoring wells, we expect to see high leakage rates for almost all of the scenarios. Thus, the time to leakage confirmation is much lower in this case. For scenario IV, where the caprock is highly fractured throughout the space, we expect a higher distribution of flux and in turn higher above zone pressure. Thus, the ability to detect a leak is also lower for this scenario. This can be seen from Table 4, where the average time to detect a leak is 6 years.

5. CONCLUSION

In this study, we simulate a caprock with semi-stochastic fracture network characteristics using FRACGEN (McKoy et al., 2006). Each model scenario is specified by fixed

statistical properties for fracture placement and size, providing the basis for simulation of multiple stochastic outcomes for each of these conceptual models. For demonstration purpose, four representative heterogeneous fractured seal types are generated, ranging from an almost impermeable caprock layer (good storage seal case) to a highly permeable caprock layer (worst storage seal case). Existing reduced order models (ROMs) are used to predict the pressure response in the Above Zone Monitoring Interval (AZMI) and flux response above the caprock for a hypothetical base case CO_2 storage scenario. The probability distributions of pressure build-up in the AZMI are modeled for each of the four caprock fracture scenarios. The modeled pressure fields are assumed to be observed with measurement errors. A Bayesian classification methodology is then developed where the pressure distributions are used as likelihood functions to compute posterior probabilities for each scenario. The Bayesian model is primarily used to calculate two parameters: firstly, the inferred probability of a given fracture scenario and secondly, the time required to distinguish above zone pressure outcomes and the associated leakage scenarios. The results indicate that with an ideal storage case where the caprock is very thick and almost impermeable, the time taken to infer that no leak is occurring is relatively short. Similarly, if the storage scenario is not ideal for CO_2 injection, i.e., the thickness of the seal is low and it is highly fractured with high permeability, then the time to infer that leakage is occurring is short. The injection rate and the thickness of the caprock have influence on the predicted caprock fracture scenario and the detection power of the simulated above zone pressure monitoring. Reduction in uncertainties of caprock geology, especially more knowledge of fracture network properties through site characterization, can lead to higher confidence in the predicted caprock fracture scenario and also improve the statistical power of detecting leakage through the caprock. Above zone pressure monitoring, combined with other monitoring techniques, such as groundwater quality monitoring, seismic monitoring, surface deformation monitoring and any other applicable monitoring techniques can be used to predict CO_2 leakage rates from the reservoir with a higher confidence.

DISCLAIMER

ACKNOWLEDGMENTS

This work was completed as part of the National Risk Assessment Partnership (NRAP) project. Support for this project came from the U.S. Department of Energy's (DOE) Office of Fossil Energy's CCS and Crosscutting Research Programs, by the Department of Civil and Environmental Engineering and the Bertucci fellowship program at Carnegie Mellon University, and by training fellowship through the Oak Ridge Institute for Science & Education (ORISE). The authors would like to thank Grant Bromhal, Mark L. McKoy, Neal W. Sams, Evgeniy M. Myshakin, Traci Rodosta, Robert Romanosky, M. Kylee Rice, and Steven Seachman of NETL and Mark Ackwiecz and Regis Conrad of U.S. DOE, Fossil Energy for their technical direction and Programmatic guidance; Liwei Zhang, Zan Wang and Ya-Mei Yang of NETL/ ORISE at NETL for their valuable technical comments.

REFERENCES

Azzolina, N. A., Small, M. J., Nakles, D. V., Bromhal, G. S., 2014. Effectiveness of subsurface pressure monitoring for brine leakage detection in an uncertain CO_2 sequestration system. Stochastic Environmental Research and Risk Assessment, 28(4), 895-909.

Benisch, K. and Bauer, S., 2013. Short-and long-term regional pressure build-up during CO_2 injection and its applicability for site monitoring. International Journal of Greenhouse Gas Control, 19, pp.220-233.

Birkholzer, J.T.; Zhou, Q. (2009) Basin-scale hydrogeologic impacts of CO_2 storage: capacity and regulatory implications. Int. J. Greenh. Gas Con. 3, 745–756.

Dhar, A., Datta, B. (2007) Multi objective design of dynamic monitoring networks for detection of groundwater pollution. J. Water Resour. Plan. Manag. 133, 329–338.

Gavalas, G.R., Shah, P.C. and Seinfeld, J.H., 1976. Reservoir history matching by Bayesian estimation. Society of Petroleum Engineers Journal, 16(06), pp.337-350.

Gerstenberger, M.C. and Christophersen, A., 2016. A Bayesian network and structured expert elicitation for Otway Stage 2C: Detection of injected CO_2 in a saline aquifer. International Journal of Greenhouse Gas Control, 51, pp.317-329.

Hoeting, J.A., Madigan, D., Raftery, A.E. and Volinsky, C.T., 1999. Bayesian model averaging: a tutorial. Statistical science, pp.382-401.

Hovorka, S.D., Meckel, T.A., Trevi˜no, R.H., (2013) Monitoring a large-volume injection at Cranfield, Mississippi—project design and recommendations. Int. J. Greenhouse Gas Control.

IPCC (Intergovernmental panel on climate change) (2005) IPCC Special Report on Carbon Dioxide Capture and Storage. Prepared by Working Group III of the Intergovernmental Panel on Climate Change [Metz, B., O. Davidson, H. C. de Coninck, M. Loos, and L. A. Meyer (eds.)]. Cambridge University Press, Cambridge, United Kingdom and New York, NY, USA, 442 pp.

Jung, Y.; Zhou, Q.; Birkholzer, J.T. (2013). Early detection of brine and CO_2 leakage through abandoned wells using pressure and surface-deformation monitoring data: concept and demonstration. Adv. Water Resources.

Lindner, E., (2015). NSealR—A Brief User's Guide for Gen3; NRAP-TRS-III-0XX-2014; NRAP Technical Report Series; U.S. Department of Energy, National Energy Technology Laboratory: Morgantown, WV; p 118.

Loaiciga, H.A. (1989) An optimization approach for groundwater quality monitoring network design. Water Resour. Res. 25, 1771–1782.

Loaiciga, H.A.; Charbeneau, R.J.; Everett, L.G.; Fogg, G.E.; Hobbs, B.F.; Rouhani, S. (1992) Review of ground-water quality monitoring network design. J. Hydraul. Eng. 118,11–37.

Mahar, P.S., Datta, B. (1997) Optimal monitoring network and ground-water-pollution source identification. J. Water Resour. Plan. Manag. 123, 199–207.

McKoy et al. (2006) FRACGEN User's Guide; U.S. Department of Energy, National Energy Technology Laboratory: Morgantown, WV.

Meyer, P.D.; Valocchi, A.J.; Eheart, J.W. (1994) Monitoring network design to provide initial detection of groundwater contamination. Water Resour. Res. 30, 2647–2659.

Meyer, P., Ye, M., Rockhold, M., Neuman, S., Cantrell, K., 2007. Combined estimation of 18 hydrogeologic conceptual model parameter and scenario uncertainty with application to 19 uranium transport at the Hanford Site 300 area. Report NUREG/CR-6940 PNNL-16396. 20 U.S. Nuclear Regulatory Commission. 124 pp.

Namhata, A.; Zhang, L.; Dilmore, R.M.; Oladyshkin, S.; Nakles, D.V. (2016) Modeling pressure changes due to migration of fluids into the Above Zone Monitoring Interval of a Geologic Carbon Storage Site, International Journal of Greenhouse Gas Control, Submitted.

NETL (National Energy Technology Laboratory), 2011. National Risk Assessment Partnership (NRAP) Project Summary, http://www.netl.doe.gov/publications/factsheets/rd/R%26D179.pdf, 15/01/2014

Nogues, J.P., Nordbotten, J.M. and Celia, M.A., 2011. Detecting leakage of brine or CO_2 through abandoned wells in a geological sequestration operation using pressure monitoring wells. Energy Procedia, 4, pp.3620-3627.

Nordbotten J, Celia M, Bachu S (2004) Analytical solutions for leakage rates through abandoned wells. Water Resources Research, 40

Pawar, R.; Bromhal, G.;.Dilmore, R.; Chu, Shaoping; Oldenburg, Curtis; Stauffer, Phil; Zhang, Yingqi; Guthrie, G. "The National Risk Assessment Partnership's Integrated Assessment Model for Carbon Storage: A Tool to Support Decision Making Amidst Uncertainty" International Journal of Greenhouse Gas Control. Volume 52, September 2016, Pages 175–189

Pruess, K., (2004). Numerical simulation of CO_2 leakage from a geologic disposal reservoir, including transitions from super-to subcritical conditions, and boiling of liquid CO_2. SPE Journal, 9(02), 237-248.

Ramaswami, A., Milford, J.B. and Small, M.J., 2005. Integrated environmental modeling: pollutant transport, fate, and risk in the environment. Wiley.

Reed, P.M.; Minsker, B.S. (2004) Striking the balance: long-term groundwater monitoring design for conflicting objectives. J. Water Resour. Plan. Manag. 130, 140–149.

Rojas, R., Feyen, L. and Dassargues, A., 2008. Conceptual model uncertainty in groundwater modeling: Combining generalized likelihood uncertainty estimation and Bayesian model averaging. Water Resources Research, 44(12).

Rojas, R., Kahunde, S., Peeters, L., Batelaan, O., Feyen, L. and Dassargues, A., 2010. Application of a multimodel approach to account for conceptual model and scenario uncertainties in groundwater modelling. Journal of Hydrology, 394(3), pp.416-435.

Sarkar, S., Toksöz, M. N., Burns, D.R. (2004), Fluid Flow Modeling in Fractures, Dept. of Earth, Atmospheric and Planetary Sciences, Massachusetts Institute of Technology, Cambridge, MA.

Snow, D.T. (1964), A parallel plate model of fractured permeable media, Ph.D. Thesis, University of California, Berkeley, USA.

Sohn, M.D., Small, M.J. and Pantazidou, M., 2000. Reducing uncertainty in site characterization using Bayes Monte Carlo methods. Journal of environmental engineering, 126(10), pp.893-902.

Strandli, C.W. and Benson, S.M., 2013. Identifying diagnostics for reservoir structure and CO_2 plume migration from multilevel pressure measurements. Water Resources Research, 49(6), pp.3462-3475.

Sun, A.Y., Painter, S.L., Wittmeyer, G.W. (2006) A robust approach for iterative contaminant source location and release history recovery. J. Contam. Hydrol. 88,181–196.

Sun, A.Y.; Nicot, J.P. (2012) Inversion of pressure anomaly data for detecting leakage at geologic carbon sequestration sites. Adv. Water Resour., 20–29.

Sun, A.Y., Nicot, J.-P., Zhang, X. (2013) Optimal design of pressure-based leakage detection monitoring networks for geologic carbon sequestration repositories. Int. J. Greenh. Gas Control 19, 251–261.

U.S. Environmental Protection Agency, (2010) Geologic CO_2 Sequestration Technology and Cost Analysis. EPA, Washington, DC.

Wang, Z.; Small, M.J. (2014) A Bayesian approach to CO_2 leakage detection at saline sequestration sites using pressure measurements. International Journal of Greenhouse Gas Control. 30, 188-196.

Wintle, B.A., McCarthy, M.A., Volinsky, C.T. and Kavanagh, R.P., 2003. The use of Bayesian model averaging to better represent uncertainty in ecological models. Conservation Biology, 17(6), pp.1579-1590.

Yang, Y.M., Small, M.J., Ogretim, E.O., Gray, D.D., Bromhal, G.S., Strazisar, B.R., Wells, A.W. (2011) Probabilistic design of a near-surface CO_2 leak detection system. Environ. Sci. Technol. 45, 6380–6387.

Yang, Y.M., Small, M.J., Ogretim, E.O., Gray, D.D., Wells, A.W., Bromhal, G.S. and Strazisar, B.R., 2012. A Bayesian belief network (BBN) for combining evidence from multiple CO_2 leak detection technologies. Greenhouse Gases: Science and Technology, 2(3), pp.185-199.

Ye, M., Pohlmann, K.F., Chapman, J.B., Pohll, G.M. and Reeves, D.M., 2010. A model□averaging method for assessing groundwater conceptual model uncertainty. Ground Water, 48(5), pp.716-728.

Yonkofski, C.M., Gastelum, J.A., Porter, E.A., Rodriguez, L.R., Bacon, D.H. and Brown, C.F., 2016. An optimization approach to design monitoring schemes for CO_2 leakage detection. International Journal of Greenhouse Gas Control, 47, pp.233-239.

Zeidouni, M. and Pooladi-Darvish, M., 2012. Leakage characterization through above-zone pressure monitoring: 2—Design considerations with application to CO_2 storage in saline aquifers. Journal of Petroleum Science and Engineering, 98, pp.69-82.

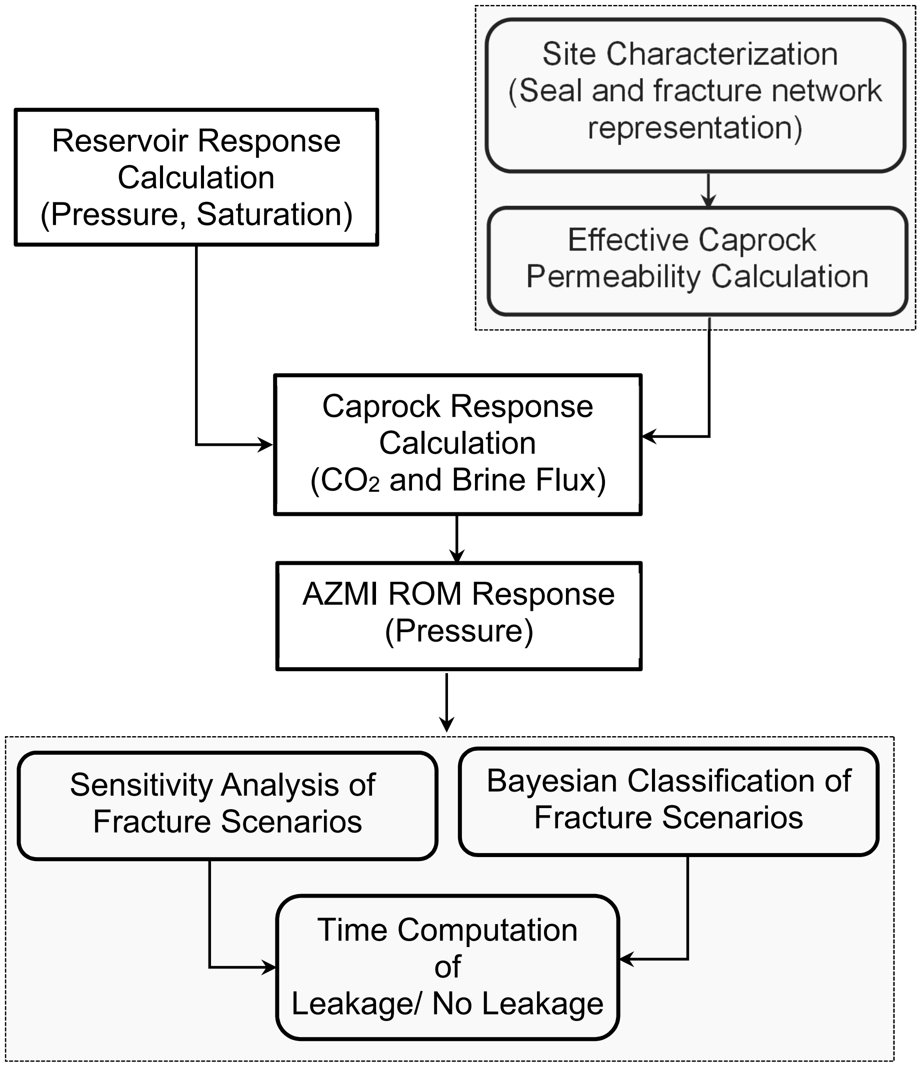

Figure 1: Schematic framework of Bayesian design for above zone pressure monitoring.

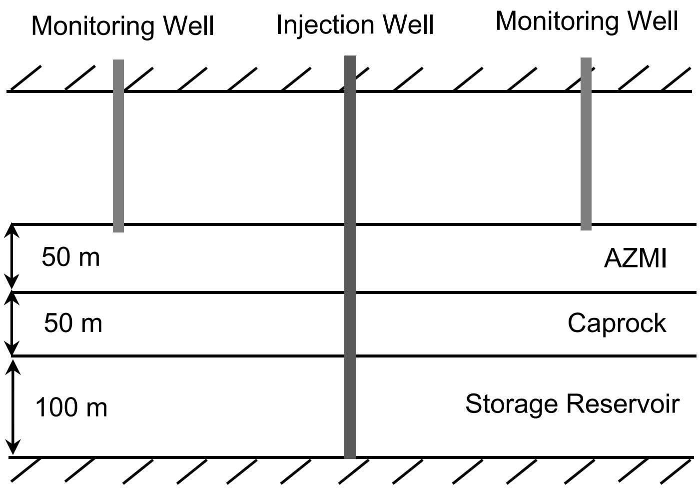

(a)

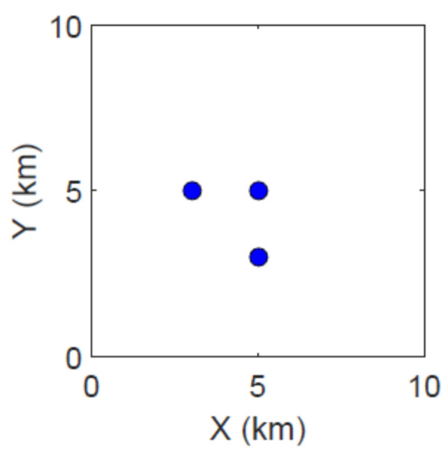

(b)

Figure 2: (a) Schematic diagram of the simplified geological model used for the base case study; (b) Top view of the spatial locations of base case monitoring wells.

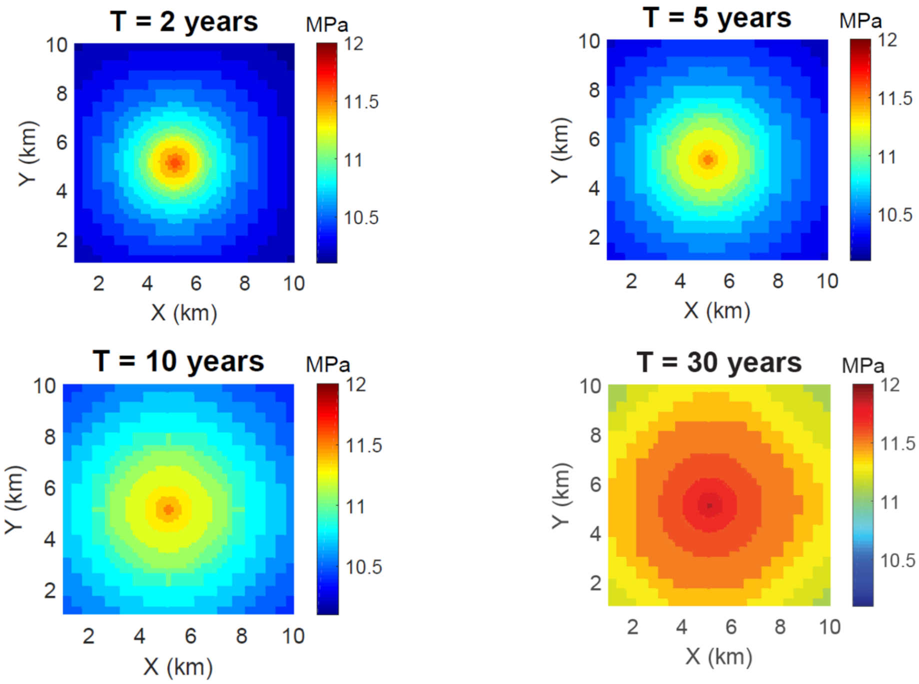

(a)

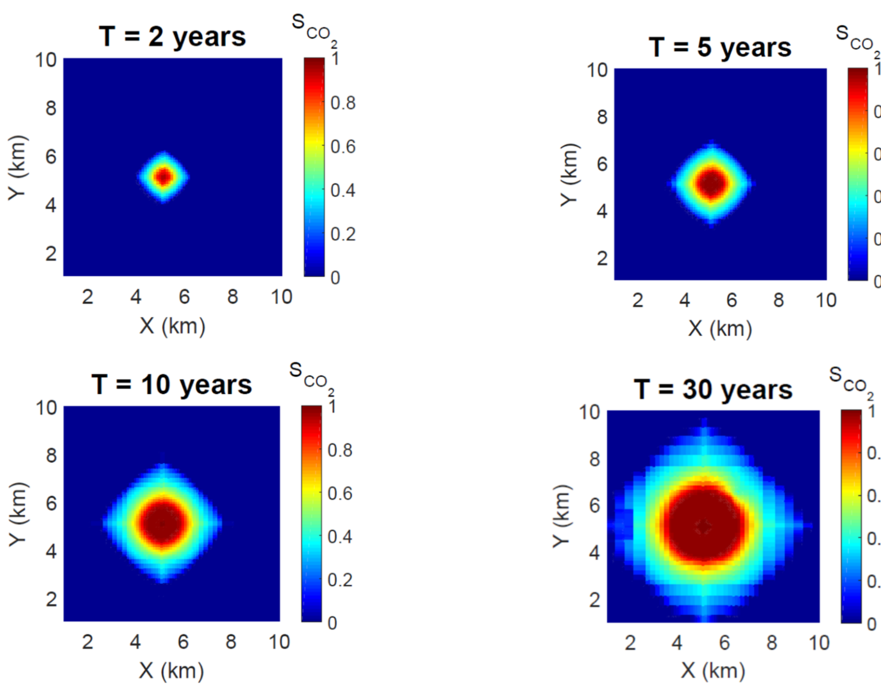

(b)

Figure 3: Evolution of (a) pressure (in MPa) and, (b) CO_2 saturation at the top of the injection reservoir at 2, 5, 10 and 30 years after the start of CO_2 injection.

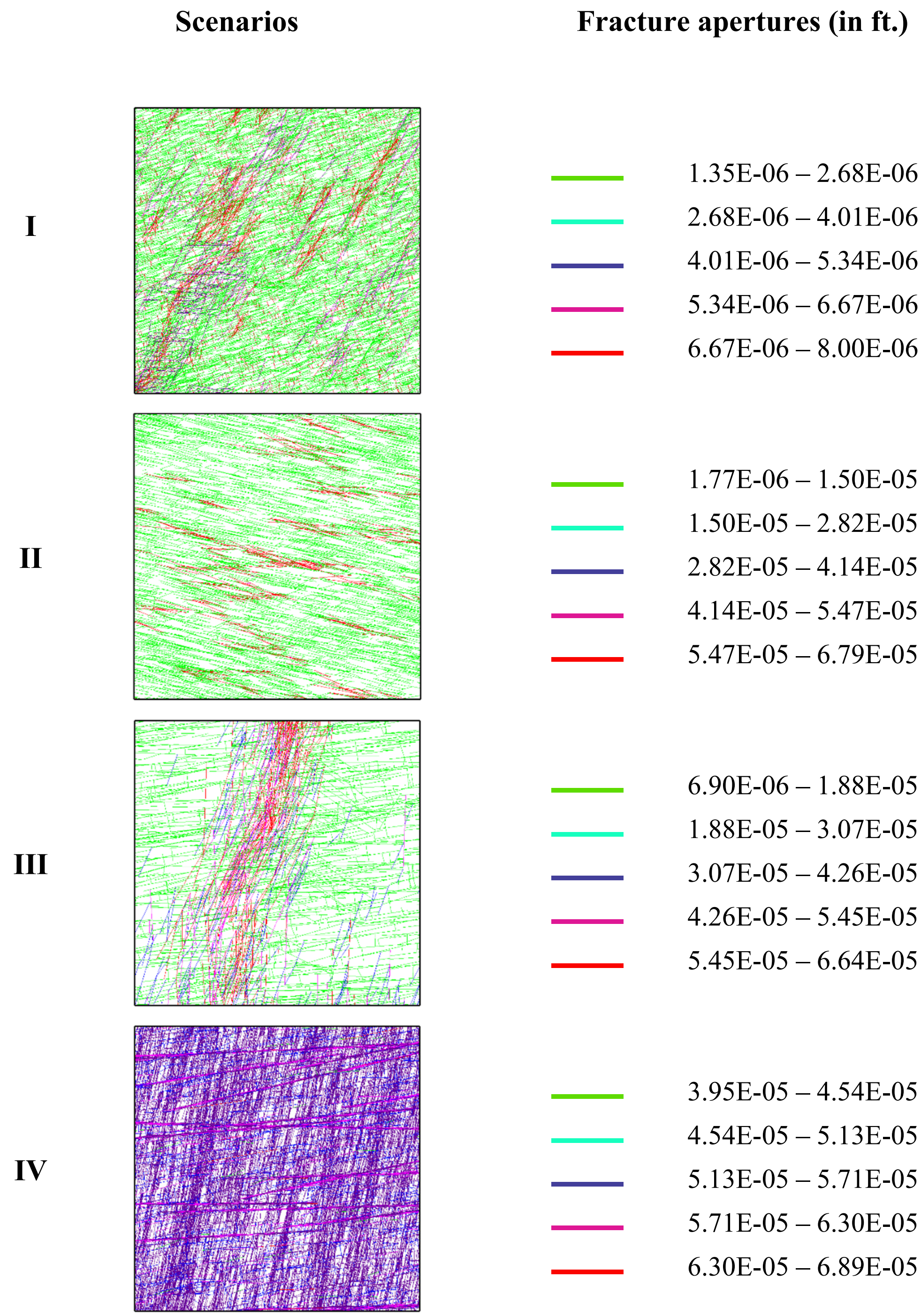

Figure 4: Graphical representation of fractured seal scenarios: (I) fractured network with low aperture; (II) densely fractured network with high aperture; (III) randomly distributed clusters of fractures with high apertures and; (IV) fractured network zone with high aperture above injection well.

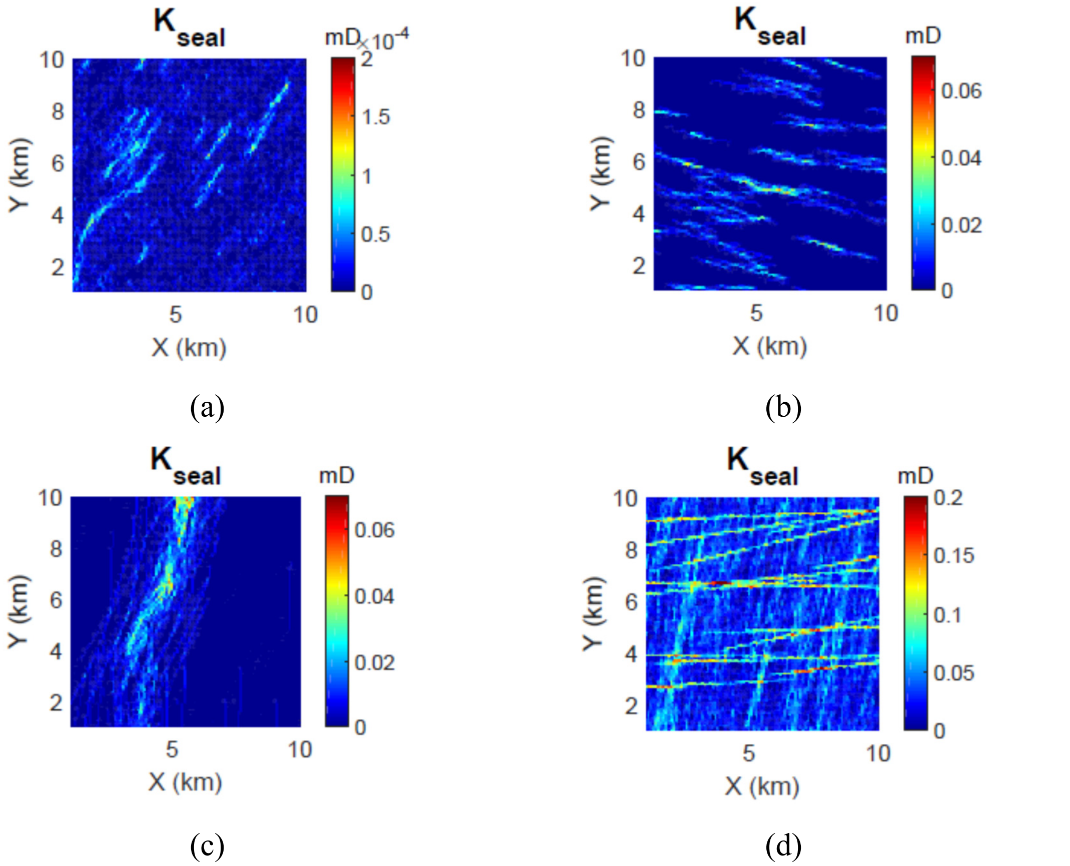

Figure 5: Calculated effective caprock permeability (in mD) for base case model with four fracture scenarios: (a) Scenario I, (b) Scenario II, (c) Scenario III and, (d) Scenario IV.

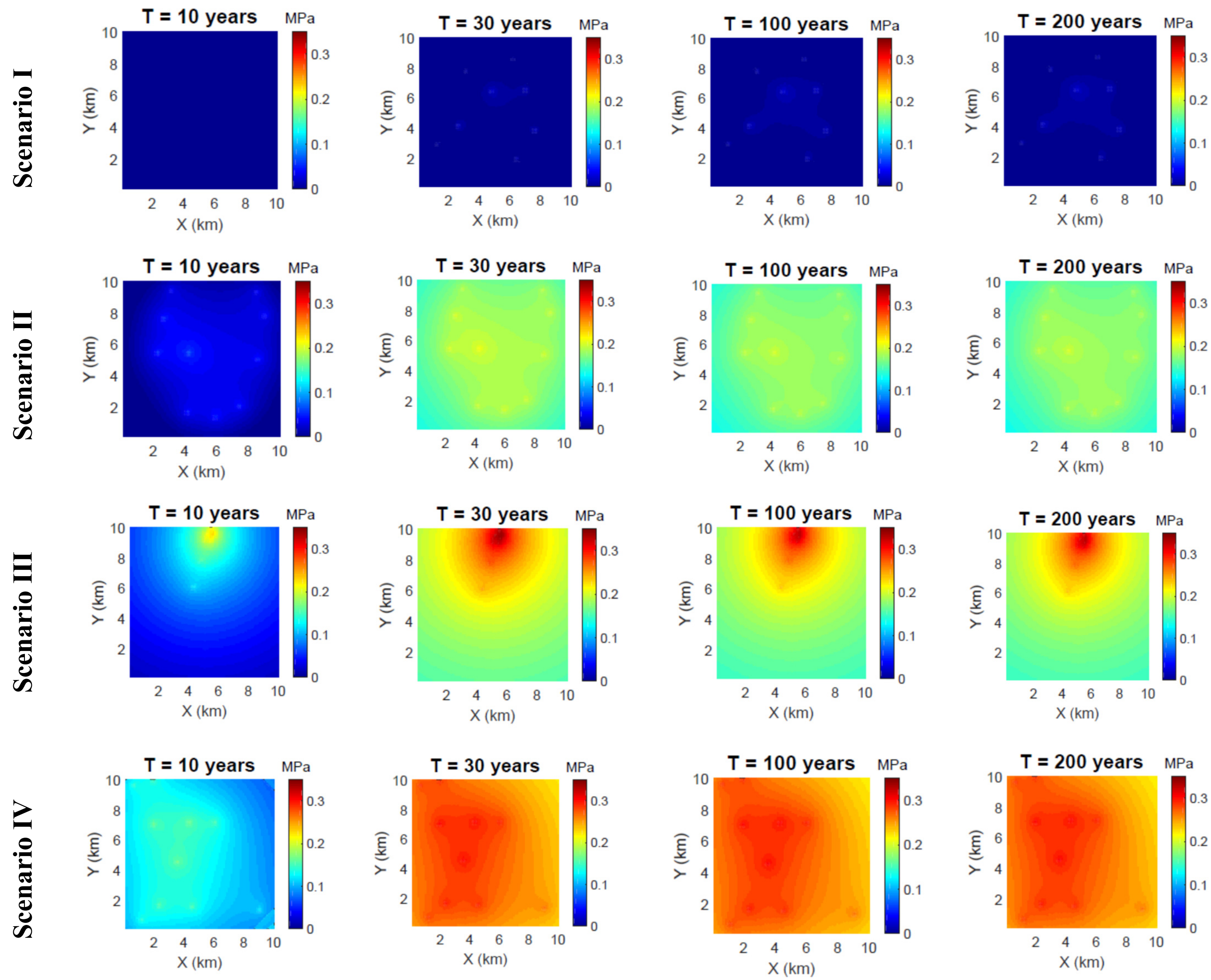

Figure 6: Change in pressure response (in MPa) at the top of AZMI through 200 years from the start of injection for the base case model with four caprock fracture scenarios.

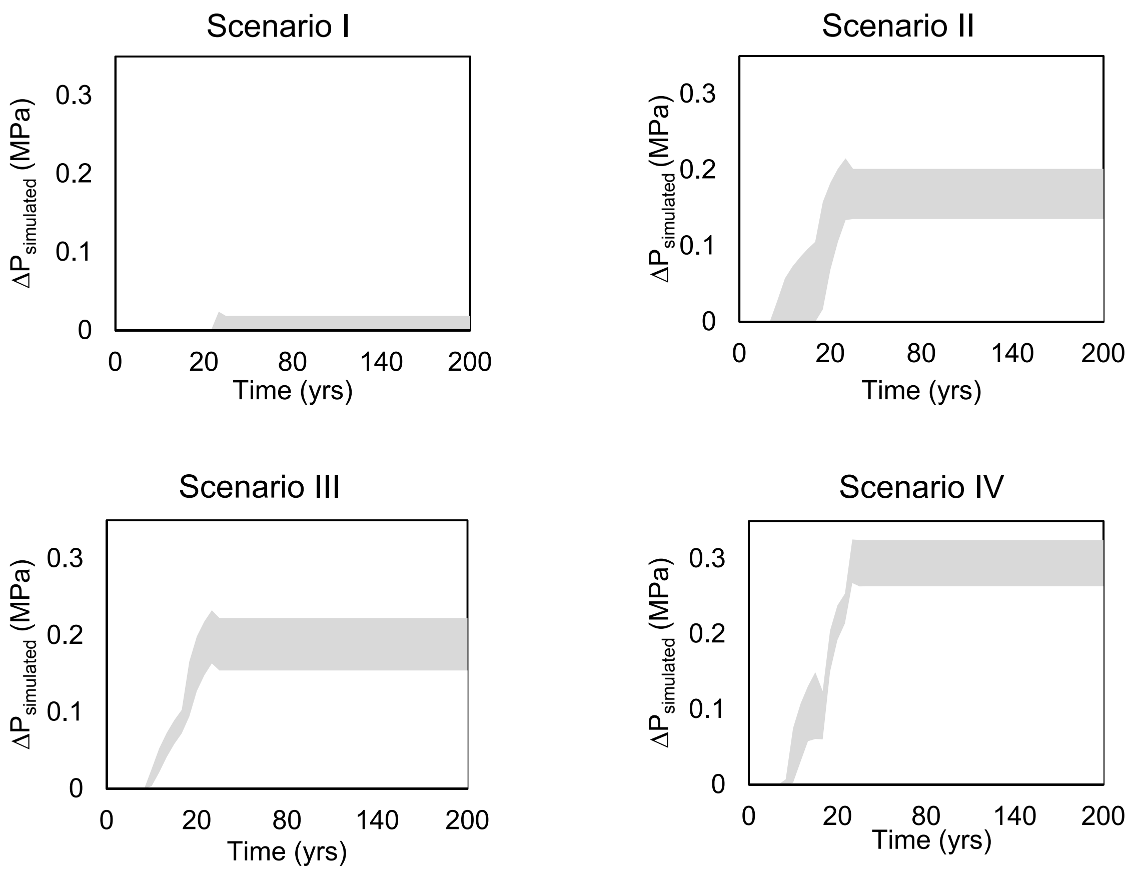

Figure 7: Range of mean of pressure build up at three designated monitoring well locations for all caprock fracture scenarios over time.

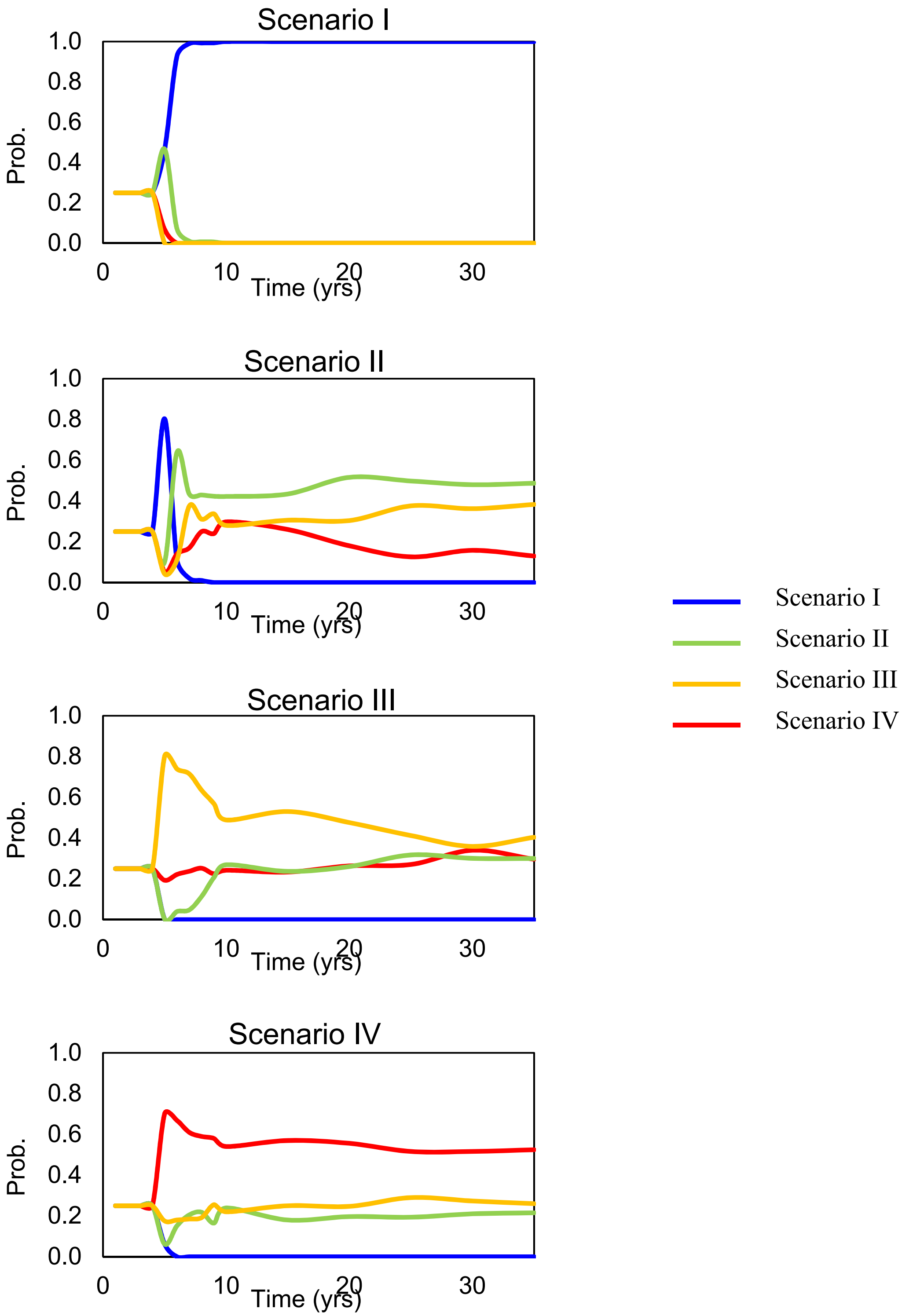

Figure 8: Posterior probabilities inferred for four different caprock fracture scenarios given a true value for a particular scenario (mentioned on top of the plots) until 35 years from the start of injection. Base case caprock thickness of 50 m and base case injection rate of 1 MT/yr.

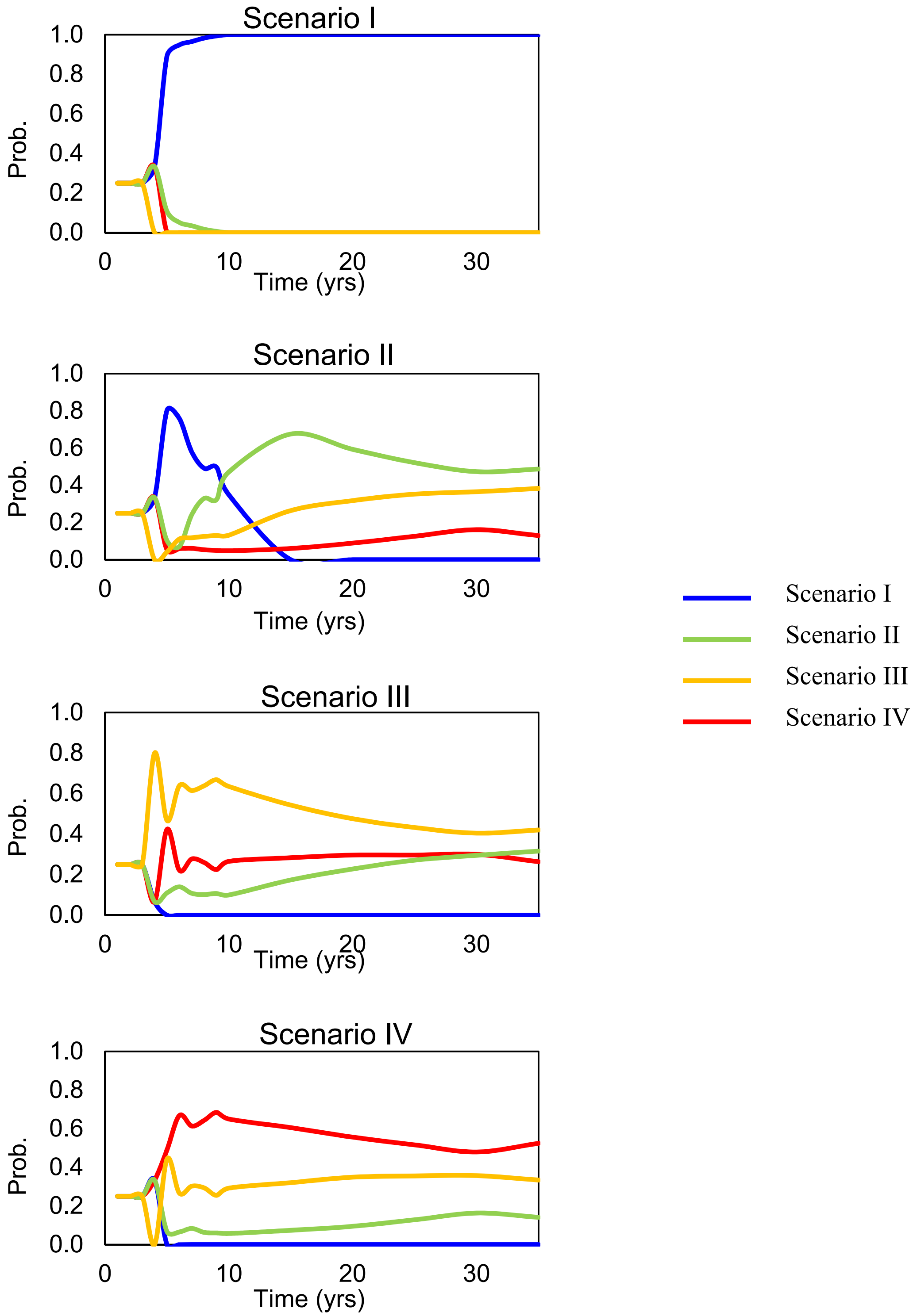

Figure 9: Posterior probabilities inferred for four different caprock fracture scenarios given a true value for a particular scenario (mentioned on top of the plots) until 35 years from the start of injection. Low caprock thickness case of 10 m and base case injection rate of 1 MT/yr.

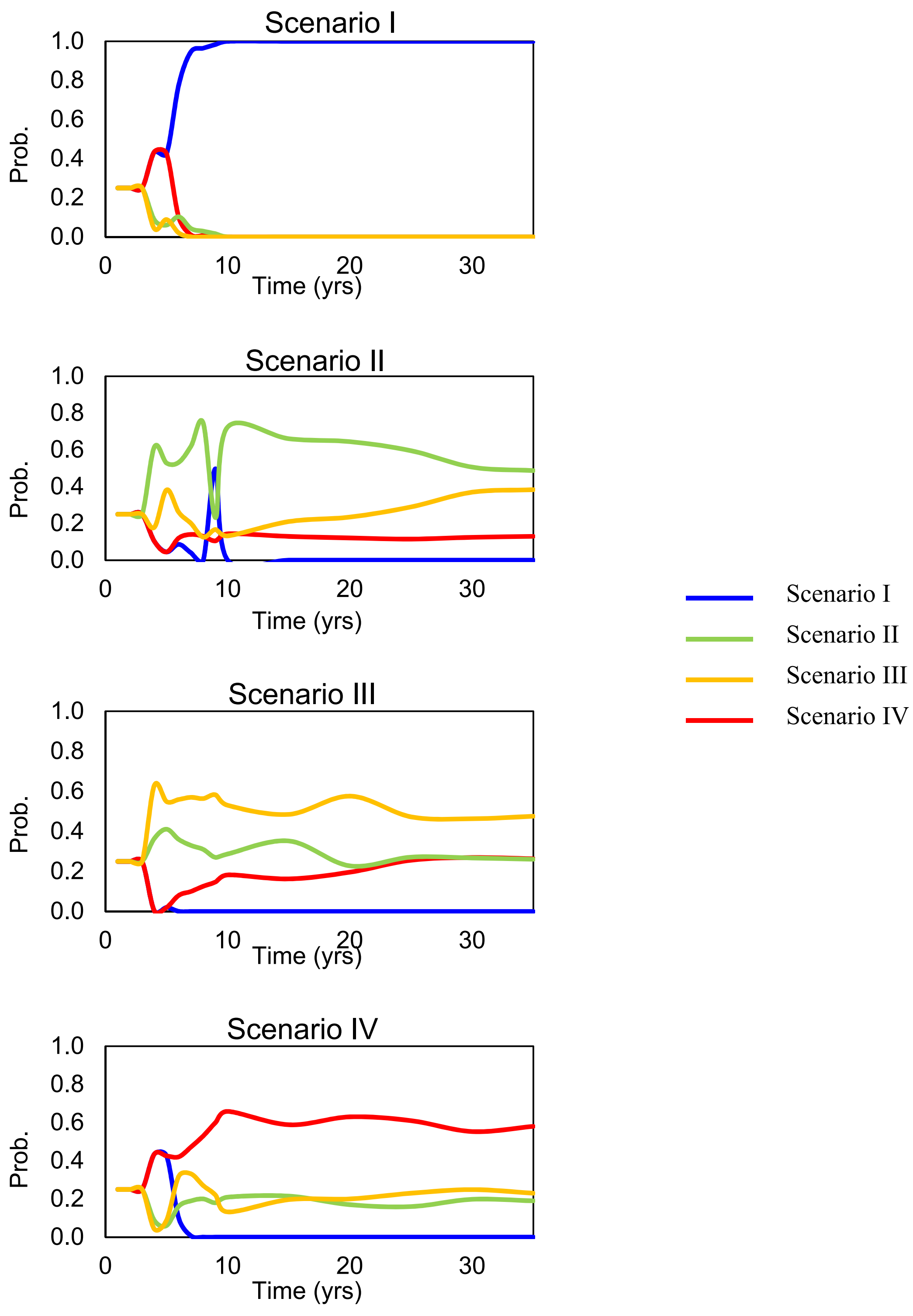

Figure 10: Posterior probabilities inferred for four different caprock fracture scenarios given a true value for a particular scenario (mentioned on top of the plots) until 35 years from the start of injection. High caprock thickness case of 100 m and base case injection rate of 1 MT/yr.

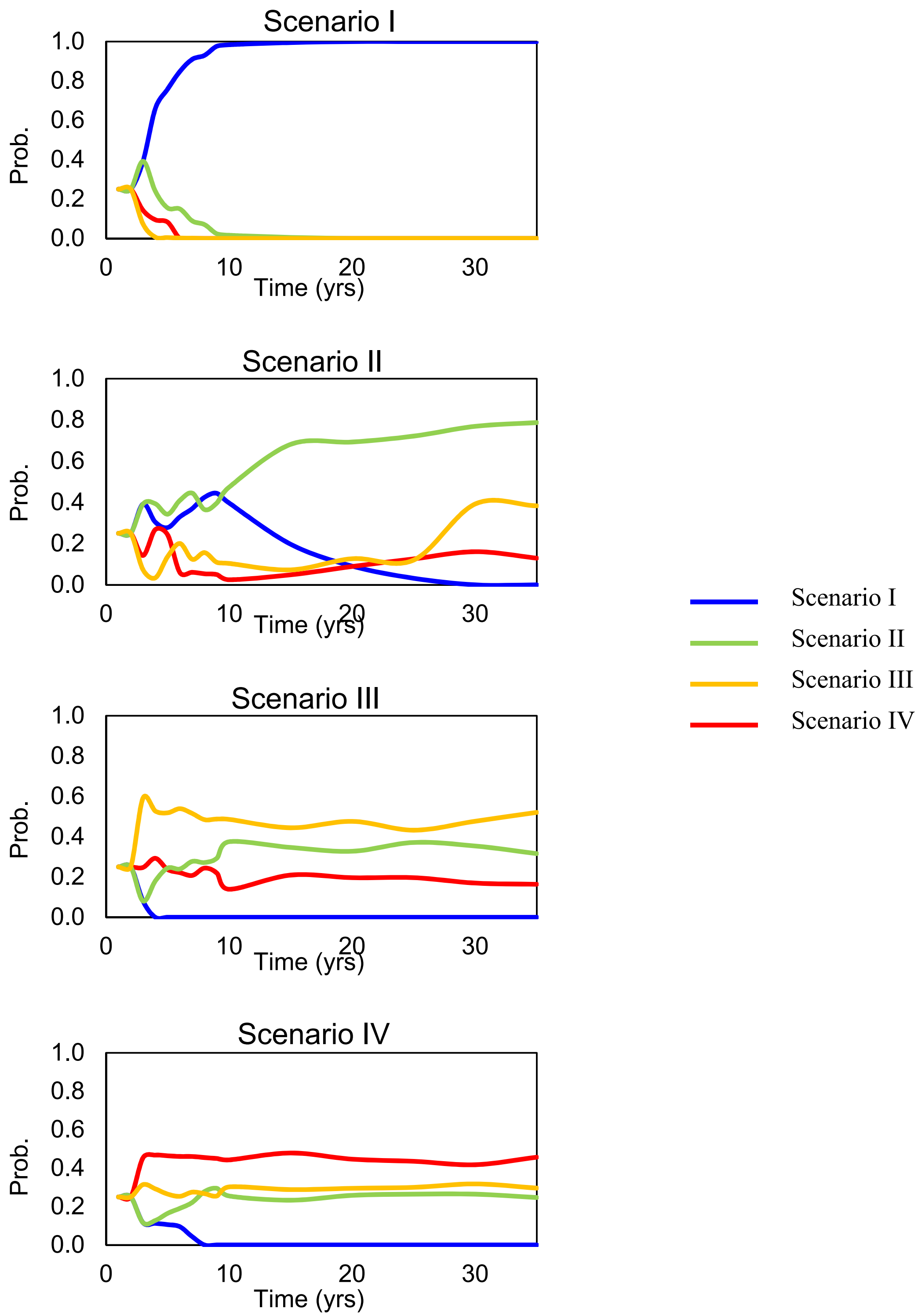

Figure 11: Posterior probabilities inferred for four different caprock fracture scenarios given a true value for a particular scenario (mentioned on top of the plots) until 35 years from the start of injection. Base case caprock thickness of 50 m and low case injection rate of 0.25 MT/yr.

.

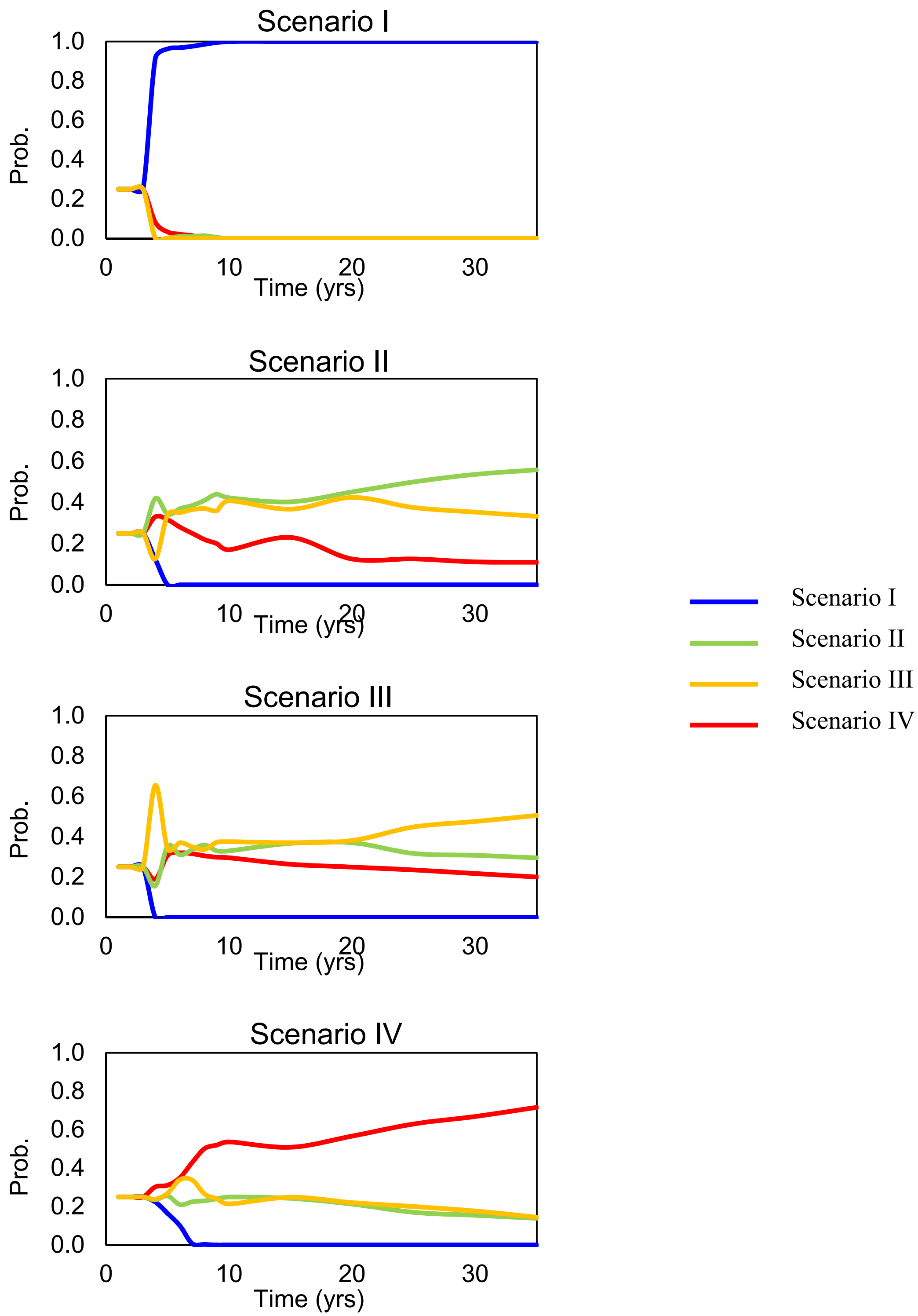

Figure 12: Posterior probabilities inferred for four different caprock fracture scenarios given a true value for a particular scenario (mentioned on top of the plots) until 35 years from the start of injection. Base case caprock thickness of 50 m and high case injection rate of 5 MT/yr.

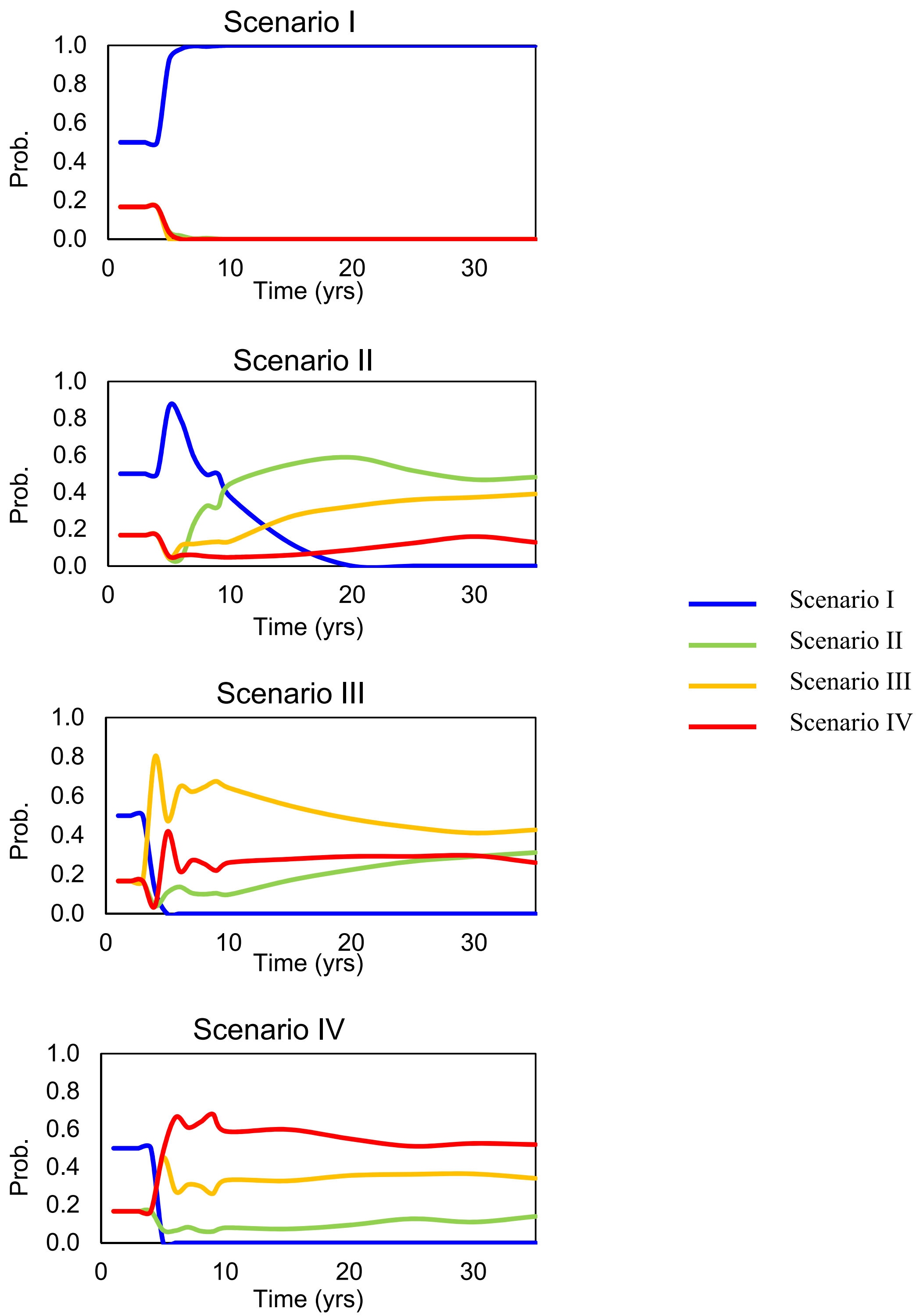

Figure 13: Posterior probabilities inferred for four different caprock fracture scenarios given a true value for a particular scenario (mentioned on top of the plots) until 35 years from the start of injection. Base case caprock thickness of 50 m and high case injection rate of 1 MT/yr. The prior probability of Scenario I is taken to be 0.50 and that of Scenarios II, III and IV to be 0.1667.

Table 1: Storage reservoir and caprock features

Parameters	Value
Density of rock	2600 kg/m^3
Initial pressure at depth =1000 m	10 MPa
Pressure gradient	10^4 Pa/m
Average temperature at caprock	50 ºC
Horizontal permeability (storage formation)	10^{-13} m^2 (0.1 D)
Vertical permeability (storage formation)	10^{-14} m^2 (0.01 D)
Salt (NaCl) mass fraction in brine	0.08
Porosity (storage formation)	0.1
Porosity (caprock)	0.05
CO_2 residual saturation	0.1
CO_2 injection period	30 years
Maximum simulation time	200 years
Domain size	10 ×10 km
Boundary condition	Open boundary